Effect of cobalt doping on the dielectric response of $Ba_{0.95}Pb_{0.05}TiO_3$ ceramics

E. Markiewicz · R. Bujakiewicz-Korońska · D. Majda ·
L. Vasylechko · A. Kalvane · M. Matczak

Abstract Dielectric response of $Ba_{0.95}Pb_{0.05}TiO_3$ ceramics doped with 0.1 and 1 wt.% of Co_2O_3, synthesized by conventional high-temperature method, was studied in wide temperature and frequency range. The temperature dependences of the real and the imaginary parts of dielectric permittivity of the ceramics were compared with those of $BaTiO_3$ and $Ba_{0.95}Pb_{0.05}TiO_3$. The addition of Co^{3+} ions results in a broadening of dielectric anomalies related to the transition to paraelectric cubic phase, and the structural transition between the tetragonal and the orthorhombic phases. At low temperatures (125–200 K) the dielectric absorption of Co-doped $Ba_{0.95}Pb_{0.05}TiO_3$ ceramics was found to exhibit relaxor-like properties. The dielectric response has been found to contain the contributions characteristic of fluctuations of the polar nanoregion boundaries and reorientations of the dipole moments between allowed directions in the nanoregions in the rhombohedral and the orthorhombic phases. The behavior speaks in favor of ordering of polar defects in the host lattice of $Ba_{0.95}Pb_{0.05}TiO_3$ in a form polar nanoregions

Keywords $Ba_{0.95}Pb_{0.05}TiO_3$ · Co-doping · Dielectric properties · Deviation from the Curie-Weiss law

E. Markiewicz (✉) · M. Matczak
Institute of Molecular Physics, Polish Academy of Science,
Smoluchowskiego 17, 60-179 Poznan, Poland
e-mail: ewamar@ifmpan.poznan.pl

R. Bujakiewicz-Korońska
Institute of Physics, Pedagogical University, Podchorążych 2,
30-084 Krakow, Poland

D. Majda
Department of Chemistry, Jagiellonian University, Ingardena 3,
30-060 Krakow, Poland

L. Vasylechko
Lviv Polytechnic National University, 12 Bandera, 79013 Lviv,
Ukraine

A. Kalvane
Institute of Solid State Physics, University of Latvia, Kengeraga 8,
LV-1063 Riga, Latvia

M. Matczak
NanoBiomedicalCentre, Adam Mickiewicz University, Umultowska
85, 61-614 Poznan, Poland

1 Introduction

$BaTiO_3$ (BT) is a classic ferroelectric which has found wide application in the electronic industry. BT ceramics is commonly used in ceramic capacitors, piezoelectric sensors or actuators as well as resistive switching elements [1–3]. The compound can exist in four phases with cubic (above 398 K), tetragonal (between 398 and 281 K), orthorhombic (between 281 and 202 K), and rhombohedral (below 202 K) crystal structure [4, 5]. All of the phases, except the cubic one, exhibit ferroelectric properties.

The structure and the dielectric properties of BT have been extensively studied for more than half a century in order to increase the dielectric permittivity and to suppress the losses [6, 7]. Nowadays the research concentrated on temperature–stable dielectrics are intensely developed [8]. Pure BT is characterized by large variations in dielectric permittivity and dielectric losses related to the structural phase transitions. In order to avoid these disadvantages, doping of pure ceramics is used. BT is known to form solid solutions with $PbTiO_3$ (PT) and an upward shift of the temperature of the tetragonal-cubic phase transition is observed with an increase of Pb content in $(1-x)BaTiO_3-xPbTiO_3$ solid solutions [9–13]. XAFS studies by Lebedev at al. [13] indicated a displacement of Pb atoms from the A lattice site in the ABO_3 perovskite structure by ~0.15 Å and a strong distortion of the oxygen environment as the main factors responsible for the appearance of ferroelectricity in the temperature range above ~400 K, that is the Curie point of pure $BaTiO_3$ [14–17]. According to the

literature data [4] the temperatures of the transitions from tetragonal to orthorombic and from orthorhombic to rhombohedral phases are lowered due to an addition of the Pb ions resulting in a broadening of the dielectric anomaly in the vicinity of room temperature.

Dielectric properties of the ceramics belonging to the $BaTiO_3$ family can be influenced by doping with the transition–metal ions. It has been found that ions with the valences smaller than 4 substituting the Ti sites exhibit acceptor character with charge deficiency compensated by doubly ionized oxygen vacancies [1, 18]. Among the 3d elements Co is known to influence the elastic and the dielectric properties of the $BaTiO_3$—based ceramics [2, 19, 20]. The addition of Co dopant up to 1 at.% results in an attenuation of mechanical losses and a smoothing of the elastic modulus anomaly [2]. The decrease of mechanical losses in the orthorhombic phase is associated with the fixing of the domain wall positions by Co^{3+} acceptor ions. Dielectric measurement by H. J. Hagemann and H. Ihrig [1] showed the lowering of the Curie point with the content of Co dopants up to 2 mol %.

The aim of this paper is to characterize the effect of Co—doping on the dielectric response of $Ba_{0.95}Pb_{0.05}TiO_3$ solid solution with very low tetragonality ($1-c/a$) and to compare the response with those of the undoped ceramics and the $BaTiO_3$ ceramics. We explore the impact of doping a material to modify the electrical properties, i.e. the relationship between the chemical and electrical properties. This relationship can be either in a good agreement with beneficial mechanical properties as pointed out in [2] or it can be coupled with lower piezoelectric activity [21]. The study of adjusting a given property can be easy adopted to the control of the another one. BT—based ceramics with 5 % PT and 0.1 % as well as 1 % Co_2O_3 doping can be very interesting from the application point of view because of the ability of a flattening the dielectric permittivity–temperature characteristic by the Co ions and a shift of the phase transition temperatures by the Pb dopants. Co^{3+} acceptor ions are incorporated into the Ti^{4+}-lattice site because of their similar ionic radii and oxygen vacancies are generated in order to compensate the valence. The resultant acceptor–oxygen vacancy dipoles in highly polarizable lattice can form either polar nanoregions (PNRs) like in ferroelectric relaxors [22–24] or can result in an internal bias which is formally equivalent to the energy difference of the dipolar defects between the accessible directions of the spontaneous polarization and affects the dielectric response [25–27]. Due to high polarizability of the ABO_3 lattice the dipolar defects polarize the neighboring part of the lattice forming the polar nanoregions the size of which is determined by temperature –dependent correlation length of the host. For low defect concentration each polar nanoregion can be treated as a noninteracting polar object characterized by a single relaxation time. At higher defect concentrations the PNRs can interact leading to more complex relaxational behavior apparent in so called ferroelectric relaxors as La substituted $PbZr_{1-x}Ti_xO_3$ family or $PbMg_{1/3}Nb_{2/3}O_3$ and $PbSc_{1/2}Nb_{1/2}O_3$

families. The relaxor-like behavior is characterized by broad and highly dispersive dielectric anomaly [22–24].

Here we present the results of detailed studies of the dielectric response of Co_2O_3 doped $Ba_{0.95}Pb_{0.05}$ ceramics to search for an influence of introduced defects on the equilibrium between the short—and the long range interactions in the host lattice. The material was characterized by X-ray diffraction (XRD) and differential scanning calorimetry (DSC).

2 Experimental

2.1 Preparation of the samples

BT—based ceramics with 5 at.% of Pb and 0.1 wt.% as well as 1 wt.% of Co_2O_3 were prepared by standard high temperature dry sintering method. Chemicals from Aldrich: Co_2O_3 (purity 99.5 %), $BaCO_3$ (99.5 %), PbO (99.0 %) and TiO_2 (99.5 %) were used. The $BaCO_3$ and TiO_2 powder were weighed in accordance to chemical formula stoichiometry to obtain $BaTiO_3$ ceramics. The BPT and BPTC ceramics were also prepared in accordance to the presumed nominal compositions. The components were mixed in ethanol and homogenized in an agate ball-mill for 24 h. After drying at 400 K, they were calcined for 2 h at the temperature of 1,493 K. Then the calcined powders were grinded, pressed under the pressure of 15 MPa at room temperature in form of pellets in diameter of 8 mm, and sintered for 2 h at 1,593 K, at ambient air. The samples were cooled in the oven from sintering temperature to room temperature for 6 h. EDX (Bruker - Quantax) studies of fractured BPTC samples show that the Pb amount lies in the range from (5.38±0.22) to (7.79±0.28) wt.%. The samples in form of discs, thickness $d=1$ mm and diameter $\phi=8$ mm, were cut off for dielectric measurements. The discs were covered with gold sputtered electrodes.

2.2 XRD studies

X-ray powder diffraction studies of the $Ba_{0.95}Pb_{0.05}TiO_3$ and $Ba_{0.95}Pb_{0.05}TiO_3+0.1\%Co_2O_3$ ceramics were performed on the laboratory Huber imaging plate Guinier camera G670 with $CuK_{\alpha1}$ radiation. The crystal structure of $Ba_{0.95}Pb_{0.05}TiO_3+0.1\%Co_2O_3$ and $Ba_{0.95}Pb_{0.05}TiO_3$ was determined from high-resolution powder diffraction with synchrotron radiation in the temperature range 298–1,173 K. Corresponding in situ high-temperature diffraction experiments were performed with powder diffractometer at the B2 beamline of synchrotron laboratory HASYLAB/DESY [28]. The program package WinCSD [29] was used in all crystallographic calculations.

2.3 DSC measurements

DSC measurements were carried out using a DSC 822^e Mettler Toledo apparatus, equipped with liquid nitrogen cooling option

Fig. 1 X-ray synchrotron powder diffraction patterns of $Ba_{0.95}Pb_{0.05}TiO_3$ (**a**) and $Ba_{0.95}Pb_{0.05}TiO_3$:0.1%Co_2O_3 (**b**); λ=0.53827 Å at RT. Experimental (*dots*) and calculated patterns, difference profiles and positions of the diffraction maxima are given
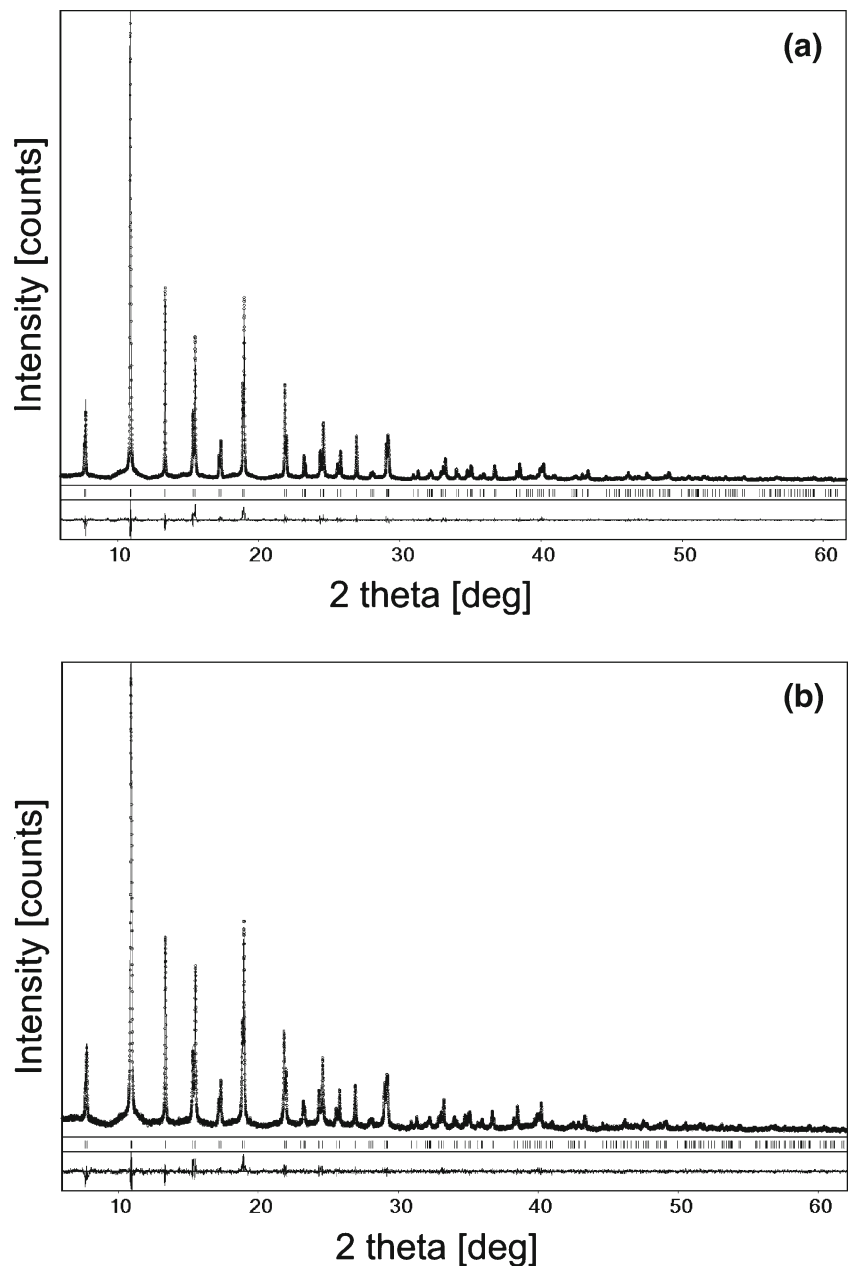
(Cryofab). The sample of studied material was hermetically sealed in an aluminum crucible and measured in temperature range from 123 K to 723 K at a heating rate of 10 K/min. The empty pan was used as a reference sample. The experiments were repeated twice to confirm the results.

2.4 Dielectric measurements

Dielectric response of the ceramic samples was studied using an Alpha-A High Performance Frequency Analyzer (Novocontrol GmbH) combined with Quatro Cryosystem for the temperature control. The sample with gold sputtered electrodes was fixed between two additional external electrodes in a sample holder

and placed into a cryostat. The measurements were performed in the temperature range from 125 K to 525 K on heating at a rate of 1 K/min. The frequency varied from 1 Hz to 1 MHz at the oscillation voltage of 1 V. The measured dielectric permittivity data were collected and evaluated by WinDETA impedance analysis software and a WinFit V 3.2. program.

3 Results and discussion

X-ray powder diffraction studies of the BPT and BPTC specimens at RT revealed tetragonal perovskite structure, similar to that of pure BT. Figure 1 shows the X-ray

Table 1 Crystallographic data for $Ba_{0.95}Pb_{0.05}TiO_3$:0.1%Co_2O_3 and $Ba_{0.95}Pb_{0.05}TiO_3$ at RT (space group $P4mm$)

Atoms, sites	x	y	z	$B_{iso/eq}$[a], Å^2	B_{11}	B_{22}	B_{33}	B_{12}, B_{13}, B_{23}
$Ba_{0.95}Pb_{0.05}TiO_3$:Co; $a = 3.99248(4)$ Å, $c = 4.03373(6)$ Å; $R_1 = 0.064$, $R_P = 0.113$								
Ba/Pb, 1a	0	0	0.0001(6)	0.751(4)	0.735(5)	B_{11}	0.783(9)	0
Ti/Co, 1b	1/2	1/2	0.4884(7)	0.75(1)	0.77(1)	B_{11}	0.70(3)	0
O1, 1b	1/2	1/2	−0.019(2)	0.83(6)	0.90(10)	B_{11}	0.69(13)	0
O2, 2c	1/2	0	0.512(2)	0.85(5)	0.94(10)	0.74(7)	0.89(8)	0
$Ba_{0.95}Pb_{0.05}TiO_3$; $a = 3.98898(9)$ Å, $c = 4.0380(1)$ Å; $R_1 = 0.068$, $R_P = 0.131$								
Ba/Pb, 1a	0	0	0.0001(9)	0.756(8)	0.71(1)	$B11$	0.84(2)	0
Ti, 1b	1/2	1/2	0.4848(9)	0.68(4)	0.73(2)	$B11$	0.57(12)	0
O1, 1b	1/2	1/2	−0.014(4)	0.75(14)	0.83(13)	$B11$	0.6(4)	0
O2, 2c	1/2	0	0.518(2)	0.8(2)	1.4(2)	0.4(1)	0.7(4)	0

[a] $B_{iso/eq} = 1/3[B_{11}(a*)^2 a^2 + \dots 2B_{23} b*c*b\,c\cos a]$; $T = exp[-1/4(B_{11}(a*)^2 h^2 + \dots 2B_{23}b*c*k\,l)]$

synchrotron powder diffraction patterns and the results of full profile Rietveld refinement obtained for both specimens. The final values of structural parameters are presented in Table 1. Besides the lattice parameters, the atomic coordinates and anisotropic displacement parameters of atoms were refined.

Examination of diffraction patterns of BPTC and BPT collected at the elevated temperatures shows that tetragonal deformation decreases with increasing temperature and completely vanishes at the temperatures higher than 453 K and 473 K for BPTC and BPT, respectively (Fig. 2). The patterns collected above this temperature show pure cubic perovskite structure. Accordingly, crystal structure parameters of the tetragonal and cubic phases of both samples have been refined in space groups $P4mm$ and $Pm\overline{3}m$, respectively. Detailed examination of the diffraction patterns of BPTC collected in the vicinities of the transition temperature revealed a coexistence of both tetragonal and cubic phases in the temperature range 383 K–423 K (inset in Fig. 2), which proves the 1st-order discontinuous character

of the phase transition in BPTC. Similar behaviour was also observed for the BPT crystal.

Simultaneous two-phase Rietveld refinement performed in space groups $P4mm$ and $Pm\overline{3}m$ confirms a coexistence of tetragonal and cubic perovskite phases in the vicinities of the transition temperatures. According to the data obtained, the amount of the tetragonal phase in BPTC decreases from 90.0 wt.% at 383 K to 20.5 wt.% at 423 K, whereas the content of the cubic phase simultaneously increases.

Figure 3 demonstrates the change in relative amounts of both perovskite phases in BPTC and BPT at the phase transitions. From these plots the temperatures of the phase transitions (the temperatures at which the amounts of tetragonal and cubic phases are equal) can be estimated as 410 K and 442 K, respectively.

Temperature dependence of the lattice parameters and cell volumes of tetragonal and cubic modifications of BPTC and BPT illustrating the first-order structural phase transition are presented in Fig. 4. The microstructural parameters of BPT
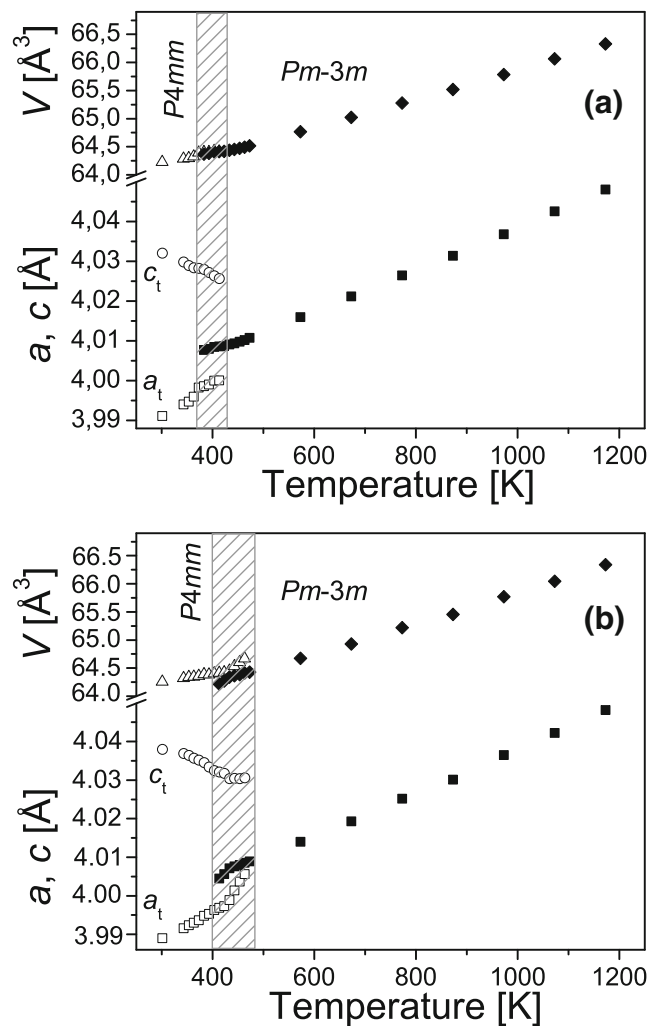
Fig. 2 Fragments of diffraction patterns collected in situ in the temperature range 343–473 K with the temperature step of 10 K (from the *bottom* to the *top*) illustrating the structural phase transition in BPTC (0.1 %)
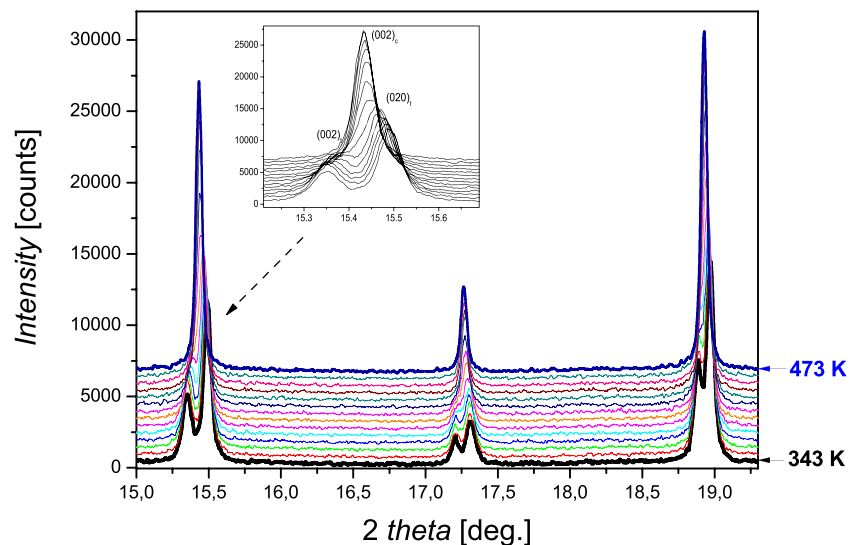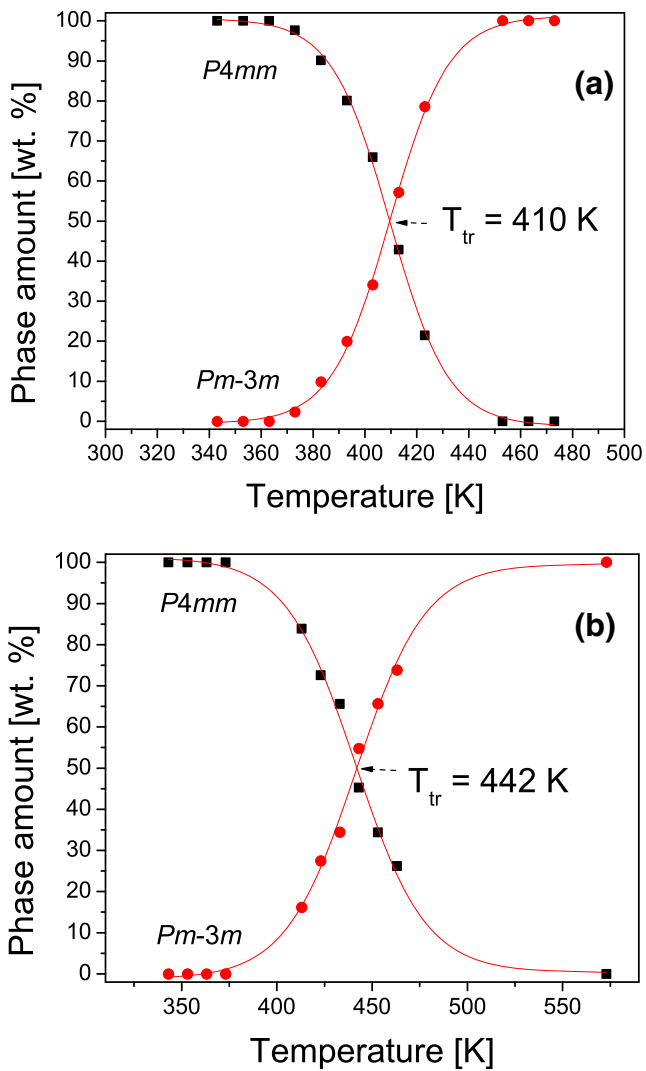
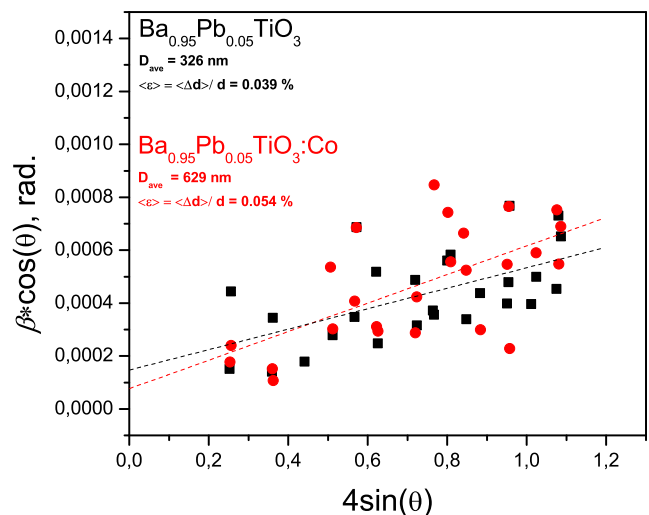Fig. 3 Refined values of the amount of tetragonal and cubic perovskite phases in BPTC (0.1 %) (a) and BPT (b) in the temperature range of the phase transitions
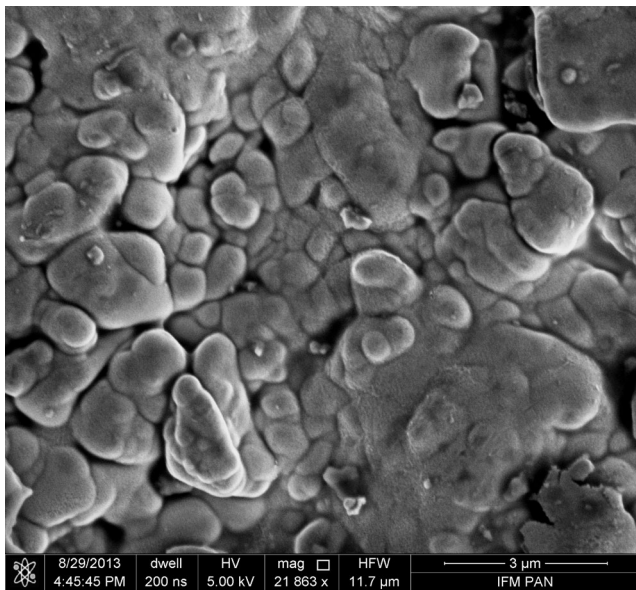

Fig. 4 Temperature dependences of the lattice parameters and cell volumes of tetragonal and cubic structures of BPTC (0.1 %) (a) and BPT (b). The areas of coexistence of both perovskite phases are *dashed*

and BPTC samples (average grain size D_{ave} and microstrains parameters $<\varepsilon> = <\Delta d>/d$) were obtained from the analysis of the broadening of X-ray powder diffraction maxima by Williamson-Hall analysis, which allows to separate the effect of size and strain broadening due to their different dependence on the scattering angle. For the BPT and BPTC (0.1 %) samples the X-ray synchrotron powder diffraction data were collected at beamline B2 synchrotron laboratory HASYLAB/DESY and the LaB_6 external standard was used for determination of instrumental broadening of the diffraction maxima. Graphical results of Williamson-Hall analysis of the microstructure of BPT and BPTC samples are presented in Fig. 5. The analysis of angular dependence of the line with (HWFM) shows that the samples are characterized by similar microstructure parameters. The average grain size was assessed to be of several hundred nm, and the average microstrains parameters $<\varepsilon>$ are between 0.04 and 0.05 %.

Fig. 5 Graphical results of the Williamson-Hall analysis of microstructure of the BPT and BPTC (0.1 %) samples by using synchrotron X-ray powder diffraction data (beamline B2 at HASYLAB/DESY, λ = 0.53821 Å, LaB_6 standard, $HWFM_{St}$ = 0.058–0.065 deg)
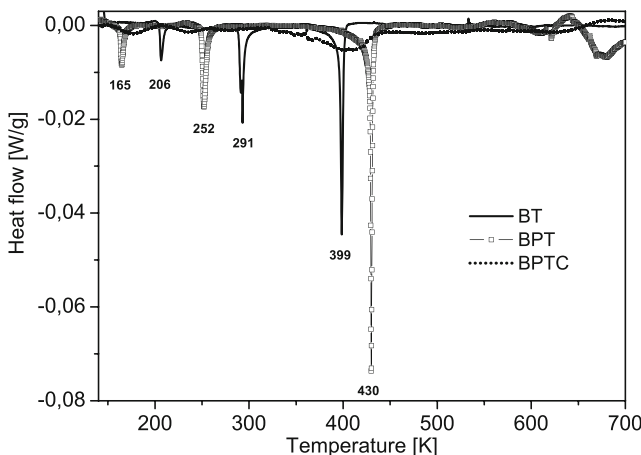
Fig. 6 SEM image of the fracture of BPTC(0.1 %) ceramic sample

Table 2 The enthalpy ΔH obtained for BT and BPT

Substance	Temperature of occurrence of peaks T_c; T_1; T_2 [K]	ΔH [J/mol]
BT	399	275
	291	163
	206	37
BPT	430	426
	252	130
	165	50

Figure 6 shows an example of the scanning electron microscope (SEM) image of a fracture of BPTC (0.1 %) sample. One can observe individual grains of average sizes of several hundred nm and their agglomerates.

The results of DSC measurements (Fig. 7) sustain the 1st-order discontinuous character of the Curie phase transition in BPT. At 430 K, one can observe a sharp peak, shifted by about 30 K towards higher temperatures in comparison with that of the BT sample. Both structural transitions: between the tetragonal and the orthorhombic phases as well as from the orthorhombic phase to the rhombohedral one in BPT are lowered by ~40 K. In the case of BPTC, all phase transitions were found to be diffused.

The enthalpy ΔH related to particular transitions in BT and BPT can be evaluated from the excess specific heat capacity using the following equation [30]:

$$\Delta H(T) = \int_{T_1}^{T_2} C_p(T)dT. \qquad (1)$$

**Fig. 7** DSC curves of BT, BPT and BPTC (0.1 %) ceramics

The values of ΔH calculated for BT and BPT are summarized in Table 2.

Figure 8 shows temperature variation of the real part of the permittivity measured at the frequency of 1 kHz for BT, BPT and BPTC ceramics. One can observe a shift of T_c towards higher temperatures by about 30 K in the case of BPT in comparison with that of BT. The addition of Co^{3+} ions results in a broadening of the dielectric anomaly and a downward shift of the Curie point. In the case of 0.1 % doping with Co_2O_3 the Curie temperature appears to be shifted by ~5.5 K and the dielectric anomaly is considerably lower than that of BPT ceramics. BPTC doped with 1 % of Co_2O_3 shows a huge dielectric anomaly shifted downwards by ~34 K with respect to that of BPT. The effect confirms the observation by H. J Hagemann and H. Ihrig [1] for $BaTiO_3$ polycrystal doped with Co^{3+}.

All investigated materials do not obey the Curie-Weiss law above T_C (Fig. 9). The temperature range ΔT_{cm} in which the deviation appears was estimated as the difference in the temperature at which the experimental point diverges from the Curie-Weiss law and the temperature of minimum of $1/\varepsilon'$. The accuracy of the ΔT_{cm} estimation we assess as ±0.2 K. This behavior points to the mechanism of the paraelectric-ferroelectric transition composed of two contributions: the displacive and the order—
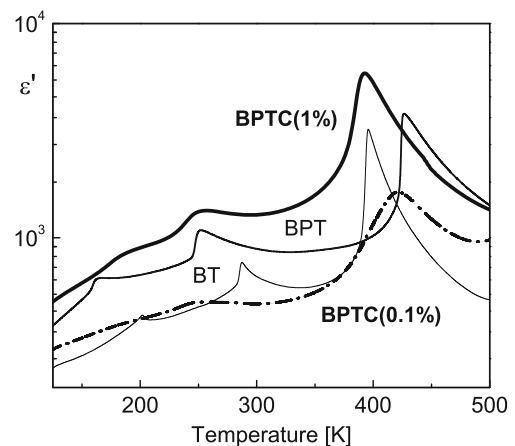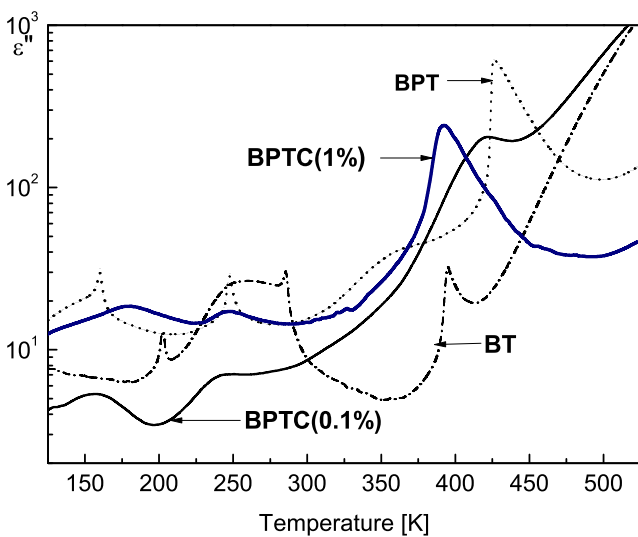

Fig. 8 Temperature dependences of real part of dielectric permittivity ε' obtained for BT, BPT, BPTC(0.1 %) and BPTC(1 %) ceramics at the frequency of 1 kHz
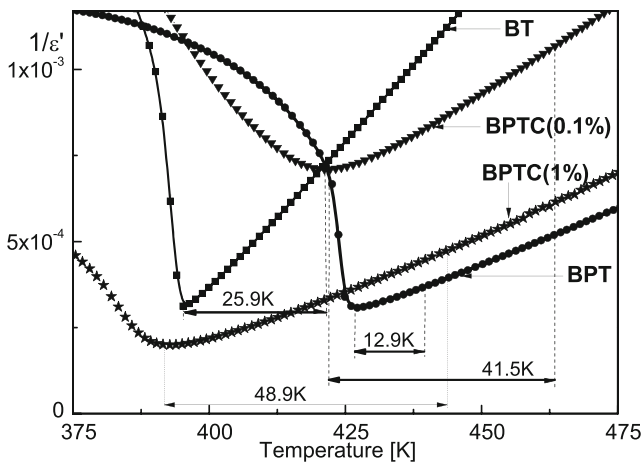
Fig. 9 Deviation degree ΔTcm from the Curie-Weiss law at the frequency of 100 kHz obtained for BT, BPT, BPTC(0.1 %) and BPTC(1 %) ceramics

disorder one. In the barium titanate the central Ti ions jump between eight equivalent <111> off-center sites inside the oxygen octahedra [31]. Fast hopping of Ti ions coexists with slow 90° flipping of displacive soft mode induced tetragonal nanodomains in the paraelectric phase [32]. As a consequence, polar clusters appear and grow when approaching the phase transition from the high temperature side. A lot of experimental methods was used to evidence both displacive and order—disorder character of the mechanism of conducting the Curie phase transition. The measurements of temperature dependence of the birefringence revealed the Δn magnitude of the order of 10^{-5} up to about 30 K above Tc due to the presence of polar clusters [33, 34]. NMR observation of the first order satellites in ^{47}Ti and ^{49}Ti spectra in the cubic phase of BaTiO$_3$ showed the

presence of nonzero quadrupole coupling at the Ti sites [35, 36] pointing to a combined displacive and order—disorder mechanism of the Curie transition. The existence of polar clusters in the paraelectric phase influences also the electrostrictive properties of BaTiO$_3$ because of the nonzero value of squared polarization P^2
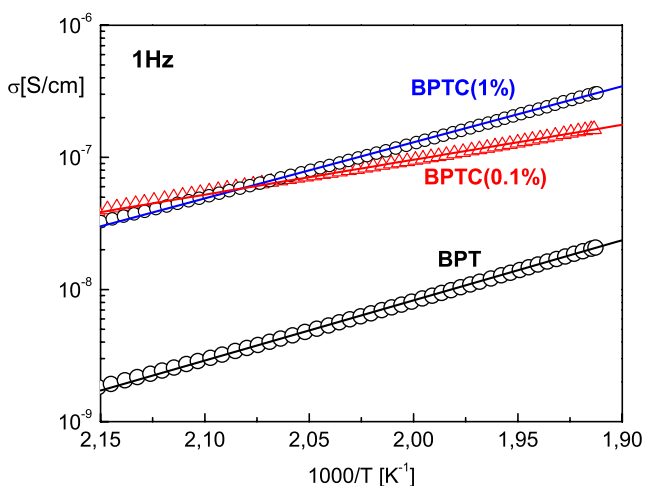

Fig. 10 Temperature dependences of imaginary part of dielectric permittivity ε'' obtained for BT, BPT, BPTC(0.1 %) and BPTC(1 %) ceramics at the frequency of 1 kHz
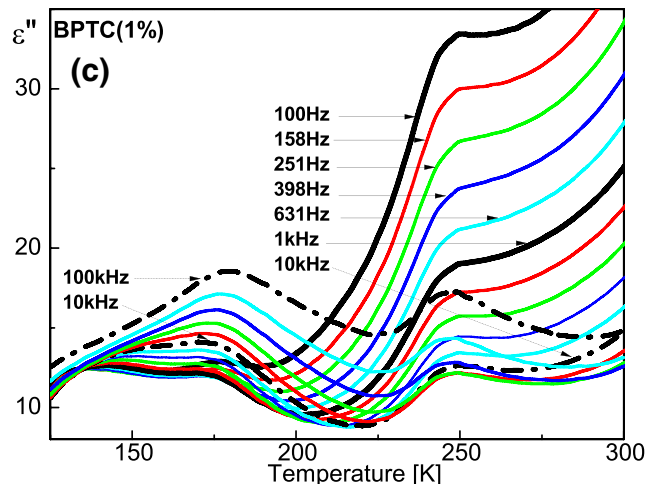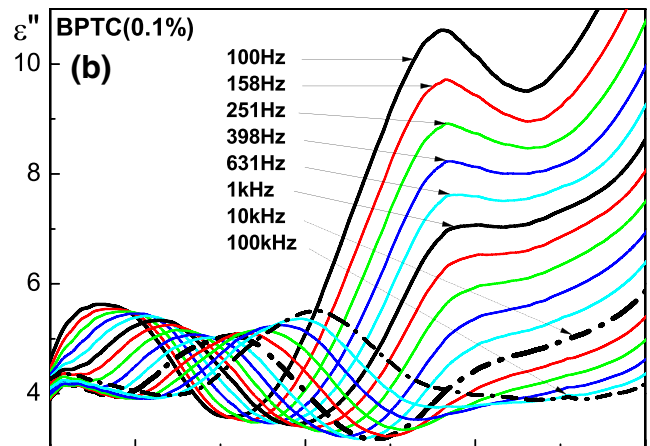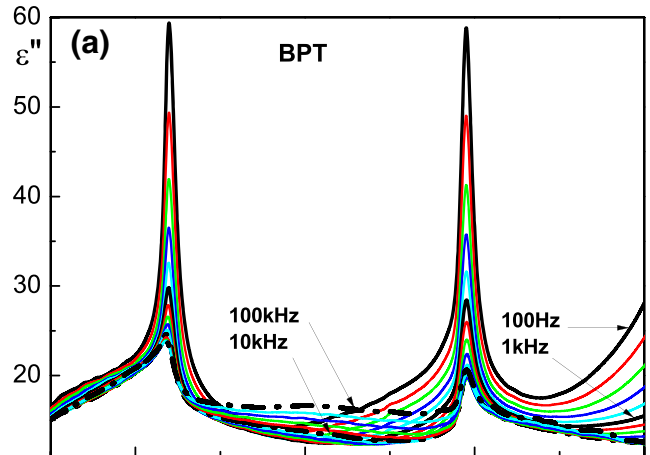
Fig. 11 Dielectric absorption of BPT, BPTC(0.1 %) and BPTC(1 %) ceramics in the low temperature range

Fig. 12 Arrhenius plots of electric conductivity of BPT, BPTC(0.1 %) and BPTC(1 %) ceramics measured at the frequency of 1 Hz in the temperature range 465 K–525 K

despite the fact that the remnant polarization is not measurable [37]. Brillouin light scattering studies [38, 39] showed anomalous changes of acoustic phonons accompanied by the appearance of quasielastic central peak on approaching Tc in the paraelectric phase. Moreover, many theoretical works based on the first-principle calculations and polarizability model [40–42] have been done to explain the deviation from Curie-Weiss behavior due to the complex dynamics of the transition.

The dielectric permittivity-temperature characteristic of BPTC shows the highest deviation degree from the Curie-Weiss law measured as $\Delta T_{cm} = T_{dev} - T_m$ [43], where T_{dev} denotes the temperature above which $1/\varepsilon'$ starts to obey the Curie-Weiss law. However the lowest deviation can be noticed for BPT. Probably, the origin of this effect is higher tetragonality ($c/a = 1.012$) observed for PBT by the XRD study (Table 1) in comparison with that of BT($c/a = 1.011$) [44, 45] and BPTC(1 %) ($c/a = 1.010$). The deviations ΔT_{cm} determined on the basis of the $1/\varepsilon'$ dependence on temperature at the frequency of 100 kHz shown in Fig. 9 are: 25.9 K, 12.9 K, 41.5 K and 48.9 K for BT, BPT, BPTC(0.1 %) and BPTC(1 %), respectively.

As seen in Fig. 8 the dielectric anomalies associated with structural transitions: from the tetragonal to the orthorhombic and from the orthorhombic to the rhombohedral phases are also influenced by doping of BT with Pb^{2+} and Co^{3+} cations. For the BPT one can observe a shift of the anomalies by about 40 K towards lower temperatures. However, the doping of BPT with Co^{3+} cations results in diffuseness of the anomaly related to the transition between the tetragonal and the orthorhombic phases. The transition from the orthorhombic phase to the rhombohedral one was not observed in the investigated temperature and frequency ranges.

Temperature dependences of the imaginary parts of dielectric permittivity ε'' shown in Fig. 10 enable further explanation of the effect of dopants on the dielectric properties of BPTC. For BPT one can observe the maxima of dielectric permittivity

ε'' bellow the Curie transition. The maxima are related to the contribution of domain wall motion to the dielectric response. The characteristic features of this process are the following: 1) it can appear only in the ferroelectric phase; 2) the relaxation frequency is strongly temperature dependent only very close to T_C and far below it approaches a value which is sample dependent; 3) the strength is strongly dependent on the quality of the material so in the case of high defect concentration it can vanish entirely [46]. In the ceramics studied, the defects can be located on the domain walls and pin their motion in the external electric field [47]. After doping with Co^{3+} cations, i.e. for BPTC one should notice the reduction of dielectric losses attributed to the domain wall motion in the orthorhombic phase. These results are in a good agreement with that obtained from the mechanical results published in [2]. We can confirm the remarks by Hardtl [48] that acceptor dopants ions fix the domain wall position.

The situation appears to be more complicated for Co^{3+} doped PBT ceramics in the low-temperature region as shown in Fig. 11. The phase transition from the rhombohedral to the orthorhombic structure apparent as $\varepsilon''(f, T)$ anomaly at ~160 K for $Ba_{0.95}Pb_{0.05}TiO_3$ disappears for cobalt doped ceramic and in the same temperature range relaxor-like relaxation processes are observed. In the case of BPTC(0.1 %) samples the maximum values of the imaginary part of dielectric permittivity ε''_{max} decrease with increasing frequency in the window 100 Hz$\leq f \leq$6 kHz whereas at higher frequencies an increase in ε''_{max} is observed and at 100 kHz its maximum appears at $T_{\varepsilon''max} \approx 203$ K. According to the theory of the dielectric response of ferroelectric relaxors [49, 50], which considers the behavior of ε'_{max} and ε''_{max} with increasing frequency, i) in the case when ε'_{max} decreases and ε''_{max} increases with increasing frequency the main contribution to the dielectric response is due to flipping of the dipole moments between allowed directions in the polar nanoregions (PNRs), ii) whereas a decrease in ε'_{max} and ε''_{max} with increasing frequency is related to the contribution of fluctuations of the boundaries of PNRs. Thus we would like to relate the dielectric response observed in the frequency range 100 Hz–6 kHz to be due mainly to the contribution of fluctuations of PNR boundaries, whereas that apparent in the frequency range 10 kHz–100 kHz to the response of the dipole moments in the dynamic polar nanoregions. The contribution of the fluctuations of the boundaries of PNRs in BPTC(1 %) is visible in the frequency window 100 Hz–1 kHz only and above 1 kHz the contribution of dipole moments flipping between allowed <111> $_{cub}$ directions in PNRs dominates in $\varepsilon''(f, T)$ behavior with $T_{\varepsilon''max} \approx 180$ K at 100 kHz.

The transition from the phase with the orthorhombic structure to that with the tetragonal symmetry appears as a narrow ε'' peak at ~247.5 K in pure $Ba_{0.95}Pb_{0.05}TiO_3$ ceramics which in Co^{3+} doped ceramics becomes considerably broadened. In BPTC(1 %) samples at frequencies higher than ~10 kHz an additional contribution to the dielectric absorption, most

probably due to the dipole moments flipping between allowed $<110>_{cub}$ directions, can be distinguished. We did not determine the activation energies E_a of the processes because the measurements were done in a narrow frequency window (2–3 frequency decades) and the results of fitting to Vogel-Fulcher equation would be loaded with a great error.

To characterize the effect of Co^{3+} doping on the high temperature electric properties of BPTC ceramics we show in Fig. 12 Arrhenius plots of electric conductivity of the ceramic samples measured at the frequency of 1 Hz in the temperature range 465 K–525 K. Doping results in an increase in the conductivity by more than one order of magnitude due to oxygen vacancies introduced to compensate the Co^{3+} valence at the B-site of the perovskite lattice. The activation energies of the oxygen vacancies migration were assessed to amount to (0.90 ± 0.05) eV, (0.84 ± 0.05) eV and (0.052 ± 0.05) eV, respectively for BPT, BPTC(1 %) and BPTC(0.1 %) ceramics. The activation energy of free oxygen vacancy migration in ferroelectric perovskite oxides has been reported to be of 0.8–1 eV [51, 52] thus we can relate the high-temperature electric conduction determined for BPT and BPTC(1 %) ceramics to the process of oxygen vacancies migration. As the distribution of the oxygen vacancies in the lattice has been considered in the tetragonal phase of the ferroelectric perovskites only [26, 50, 52] it is hard to discuss the lowering of the activation energy for BPTC(0.1 %) since the energy landscape of oxygen and probably also Pb vacancies is uncertain.

4 Conclusions

A new ceramic material (BPTC) was proposed for applications in the electronic industry and its dielectric properties were investigated. The experiment confirmed that the content of Pb^{2+} ions substituting the Ba^{2+} ions in A—site is very useful tool to control the Curie temperature. From the application point of view it is very promising the effect of reduction of high dielectric losses related to the structural phase transition in BPTC due to doping with Co^{3+} ions. It should be mentioned that Pb^{2+} and Co^{3+} doping of $BaTiO_3$ results in a diffusiveness and broadening of the ferroelectric—paraelectric phase transition. Moreover, we found that BPTC exhibits relaxor-like behavior in the low-temperature range, from 125 to 225 K which speaks in favour of the polar nanoregions, originating from the presence of Co^{3+} acceptor-oxygen vacancy dipoles in highly polarizable lattice, to be responsible for the modification of the physical properties. Moreover, the dielectric relaxation processes apparent in the rhombohedral and the orthorhombic phases of Co-doped BPT ceramics enabled to distinguish the contribution to the dielectric response of fluctuations of polar nanoregion boundaries and that of dipole moments reorientation between the allowed directions in the polar nanoregions. As the Co-doping has been reported to decrease the mechanical losses

and to smooth the elastic modulus anomaly in BT based ceramics [2] we believe to open the discussion on the effect of a well defined polar heterogeneity at the nanoscale in oxide perovskites on the anomalies of physical properties at the structural phase transitions.

References

1. H.J. Hagemann, H. Ihring, Valence change and phase stability of 3*d*-doped $BaTiO_3$ annealed in oxygen and hydrogen. Phys. Rev. B **20**, 3871–3878 (1979)
2. B.L. Cheng, M. Gabbay, W. Jr Duffy, G. Fantozzi, Mechanical loss and Young's modulus associated with phase transitions in barium titanate based ceramics. J. Mater. Sci. **31**, 4951–4955 (1996)
3. K. Uchino, *Ferroelectric Devices* (Marcell Dekker, Inc., New York - Basel, 2000), pp. 105–118
4. Landolt-Börnstein, *Numerical Data and Functional Relationships in Science and Technology, Vol. III/16a* (Springer, Berlin, 1981), p. 421
5. Y.L. Li, L.E. Cross, L.Q. Chen, A phenomenological thermodynamic potential for $BaTiO_3$ single crystals. J. Appl. Phys. **98**, 064101-1-4 (2005)
6. R.F. Blunt, W.F. Love, The dielectric properties of Barium Titanate at low temperatures. Phys. Rev. **76**, 1202–1204 (1949)
7. G. Arlt, D. Hennings, G. de With, Dielectric properties of fine–grained barium titanate ceramics. J. Appl. Phys. **58**, 1619–1625 (1985)
8. H. Kishi, Y. Okino, M. Honda, Y. Iguchi, M. Imaeda, Y. Takahashi, H. Ohsato, T. Okuda, The effect of MgO and rare-earth oxide on formation behavior of core-shell structure in $BaTiO_3$. Jpn. J. Appl. Phys. **36**, 5954–5957 (1997)
9. J.F. Meng, B.K. Rai, R.S. Katiyar, G.T. Zou, Study of visible emission and phase transition in nanocrystalline $A_{(1-x)}A'_xTiO_3$ systems. Phys. Lett. A **229**, 254–258 (1997)
10. A.V. Myasoedov, S.R. Syrtsov, Positive temperature coefficient of resistance in the lead-containing ceramic barium titanate. Tech. Phys. **42**, 1097–1098 (1997)
11. I.V. Lisnevskaya, I.A. Bobrova, E.A. Bikyashev, T.G. Lupeiko, Interfacial reactions and properties of $Y_3Fe_5O_{12}/Ba_{1-x}Pb_xTiO_3$ composites. Inorg. Mater. **42**, 1147–1151 (2006)
12. J. Brančin, L. Medveck, Influence of mechanical activation of precursors on the structure and properties of donor doped $Ba_{0.95}Pb_{0.05}TiO_3$ ceramics. J. Mater. Sci. Lett. **21**, 55–59 (2002)
13. A.I. Lebedev, I.A. Sluchinskaya, A. Erko, A.A. Veligzhanin, A.A. Chernyshov, XAFS studies of the local environment of Pb impurity atoms in barium, strontium, and calcium titanates. Phys. Solid State **51**, 991–997 (2009)

14. Landolt-Börnstein, *Numerical Data and Functional Relationship in Science and Technology, Vol. III/28a* (Springer, Berlin - Heidelberg, 1990), p. 228

15. J.H. Kim, S.H. Yoon, Y.H. Han, Effects of Y_2O_3 addition on electrical conductivity and dielectric properties of Ba-excess $BaTiO_3$. J. Eur. Ceram. Soc. **27**, 1113–1116 (2007)

16. Y. Park, H.G. Kim, The microstructure analysis of cerium – modified Barium Titanate having core-shell structured grains. Ceram. Int. **23**, 329–336 (1997)

17. H. Takeda, H. Harinaka, T. Shiosaki, M.A. Zubair, C. Leach, R. Freer, T. Hoshina, T. Tsurumi, Fabrication and positive temperature coefficient of resistivity properties of semiconducting ceramics based on the $BaTiO_3$–$(Bi_1/2K_{1/2})TiO_3$ system. J. Eur. Ceram. Soc. **30**, 555–559 (2010)

18. R.A. Serway, W. Berlinger, K.A. Müller, R.W. Collins, Electron paramagnetic resonance of three manganese centers in reduced $SrTiO_3$. Phys. Rev. B **16**, 4761–4768 (1977)

19. W. Li, J. Qi, Y. Wang, L. Li, Z. Gui, Doping behaviors of Nb_2O_5 and Co_2O_3 in temperature stable $BaTiO_3$-based ceramics. Mat. Lett. **57**, 1–5 (2002)

20. Q. Li, J. Qi, Y. Wang, Z. Gui, L. Li, Improvement of temperature-stable $BaTiO_3$-based dielectrics by addition of Li_2CO_3 and Co_2O_3. J. Eur. Ceram. Soc. **21**, 2217–2220 (2001)

21. S. Zhang, J.B. Lim, H.J. Lee, T.R. Shrout, Characterization of hard piezoelectric lead-free ceramics. IEEE Trans. Ultrason. Ferroelectr. Freq. Control **56**, 1523–1527 (2009)

22. L.E. Cross, Relaxor ferroelectrics: an over view. Ferroelectrics **151**, 305–320 (1994)

23. A.A. Bokov, Z.-G. Ye, Recent progress in relaxor ferroelectrics with perovskite structure. J. Mater. Sci. **41**, 31–52 (2006)

24. G.A. Samara, The relaxational properties of compositionally disordered ABO_3 perovskites. J. Phys. Condens. Matter **15**, R367–R411 (2003)

25. M.E. Lines, A.M. Glass, *Principle and application of ferroelectric and related materials* (Clarendon, Oxford, 1977)

26. G. Arlt, H. Neumann, Internal bias in ferroelectric ceramics: origin and time dependence. Ferroelectrics **87**, 109–120 (1988)

27. R. Bujakiewicz-Korońska, A. Kalvane, Y. Zhydachevskii, B. Garbarz-Glos, W. Śmiga, L. Vasylechko, J. Czerwiec, A. Suchocki, A. Kamińska, W. Piekarczyk, Physical Properties of Ba0.95Pb0.05TiO3+0.1%Co2O3. Ferroelectrics **436**, 62–71 (2012)

28. M.C. Baehtz, H. Ehrenberg, H. Fuess, The synchrotron powder diffractometer at beamline B2 at HASYLAB/DESY: status and capabilities. J. Synchrotron Radiat. **11**, 328–334 (2004)

29. L.G. Akselrud, P.Y. Zavalij, Y. Grin, V.K. Pecharsky, B. Baumgartner, E. Wölfel, Use of the CSD programme package for structure determination from powder data. Mater. Sci. Forum **133**, 335–340 (1993)

30. G.W.H. Höhne, W.F. Hemminger, H.-J. Flammersheim, *Differential Scanning Calorimetry* (Springer, Berlin Heidelberg, 2003), p. 140

31. R. Pirc, R. Blinc, Off-center Ti model of barium titanate. Phys. Rev. B **70**, 134107-1-8 (2004)

32. A. Bussmann-Holder, H. Beige, G. Völkel, Precursor effects, broken local symmetry, and coexistence of order–disorder and displacive dynamics in perovskite ferroelectrics. Phys. Rev. B **79**, 184111-1-6 (2009)

33. A. Ziębińska, D. Rytz, K. Szot, M. Górny, K. Roleder, Birefringence above Tc in single crystals of barium titanate. J. Phys. Condens. Matter **20**, 142202-1-5 (2008)

34. M. Takagi, T. Ishidate, Anomalous birefringence of cubic $BaTiO_3$. Solid State Commun. **113**, 423–426 (2000)

35. B. Zalar, V.V. Laguta, R. Blinc, NMR evidence for the coexistence of order–disorder and displacive components in Barium Titanate. Phys. Rev. Lett. **90**, 037601-1-4 (2003)

36. B. Zalar, A. Lebar, J. Seliger, R. Blinc, NMR study of disorder in $BaTiO_3$ and $SrTiO_3$. Phys. Rev. B **71**, 064107-1-12 (2005)

37. K. Wieczorek, A. Ziębińska, Z. Ujma, K. Szot, M. Górny, I. Franke, J. Koperski, S. Soszyński, K. Roleder, Electrostictive and piezoelectric effect in $BaTiO_3$ and $PbZrO_3$. Ferroelectrics **336**, 61–67 (2006)

38. J.H. Ko, S. Kojima, T.Y. Koo, J.H. Jung, C.J. Won, N.J. Hur, Elastic softening and central peaks in $BaTiO_3$ single crystals above the cubic-tetragonal phase-transition temperature. Appl. Phys. Lett. **93**, 102905-1-3 (2008)

39. J.H. Ko, T.H. Kim, K. Roleder, D. Rytz, S. Kojima, Precursor dynamics in the ferroelectric phase transition of barium titanate single crystals studied by Brillouin light scattering. Phys. Rev. B **84**, 094123-1-9 (2011)

40. R. Migoni, H. Bilz, D. Bäuerle, Origin of raman scattering and ferro-electricity in oxid perovskites. Phys. Rev. Lett. **37**, 1155–1158 (1976)

41. I. Ponomareva, L. Bellaiche, T. Ostapchuk, J. Hlinka, J. Petzelt, Terahertz dielectric response of cubic $BaTiO_3$. Phys. Rev. B **77**, 012102-1-4 (2008)

42. H. Bilz, G. Benedek, A. Bussmann-Holder, Theory of ferroelectricity: the polarizability model. Phys. Rev. B **35**, 4840–4849 (1987)

43. J. Suchanicz, G. Stopa, K. Konieczny, D. Wcislo, M. Dziubaniuk, J. Rymarczyk, Uniaxial pressure effect on the dielectric properties of the $BaTiO_3$ single crystals. Ferroelectrics **366**, 3–10 (2008)

44. H.D. Megaw, Crystal structure of double oxides of the perovskite type. Proc. Phys. Soc. **58**, 133–152 (1946)

45. Y. Yoshimura, M. Morioka, A. Kojima, N. Tokunaga, T. Koganezawa, K. Tozaki, Reinterpretation of the unit cell evolution of BaT_iO_3. Phys. Lett. A **367**, 394–401 (2007)

46. C. Pawlaczyk, Domain wall dielectric response in the phase transition region in some ferroelectric. Ferroelectrics **140**, 127–132 (1993)

47. K. Carl, K.H. Hardtl, Electrical after-effects in $Pb(Ti,Zr)O_3$ ceramics. Ferroelectrics **17**, 473–486 (1978)

48. K.H. Hardtl, Electrical and mechanical losses in ferroelectric ceramics. Ceram. Int. **8**, 121–127 (1982)

49. A.A. Bokov, Z.-G. Ye, Low-frequency dielectric spectroscopy of the relaxor ferroelectric $Pb(Mg_{1/3}Nb_{2/3})O_3$-$PbTiO_3$. Phys. Rev. B **65**, 144112-1-10 (2002)

50. A.A. Bokov, Z.-G. Ye, Dielectric relaxation in relaxor ferroelectrics. J. Adv. Diel. **2**, 1241010-1-24 (2012)

51. C.H. Park, Microscopic study on migration of oxygen vacancy in ferroelectric perovskite oxide. J. Phys. Soc. **42**, S1420–S1424 (2003)

52. P. Erhart, R.-A. Eichel, P. Träskelin, K. Albe, Association of oxygen vacancies with impurity metal ions in lead titanate. Phys. Rev. B **76**, 174116-1-12 (2007)